

# Calumenin, a multiple EF-hands $\text{Ca}^{2+}$ -binding protein, interacts with ryanodine receptor-1 in rabbit skeletal sarcoplasmic reticulum ☆

Dai Hyun Jung, Sang Hyun Mo, Do Han Kim \*

*Department of Life Science, Gwangju Institute of Science and Technology, Gwangju 500-712, Republic of Korea*

Received 14 February 2006

Available online 28 February 2006

## Abstract

Calumenin is a multiple EF-hand  $\text{Ca}^{2+}$ -binding protein located in endo/sarcoplasmic reticulum of mammalian tissues. In the present study, we cloned two rabbit calumenin isoforms (rabbit calumenin-1 and -2, GenBank Accession Nos. [AY225335](#) and [AY225336](#), respectively) by RT-PCR. Both isoforms contain a 19 aa N-terminal signal sequence, 6 EF-hand domains, and a C-terminal ER/SR retrieval signal, HDEF. Both calumenin isoforms exist in rabbit cardiac and skeletal muscles, but calumenin-2 is the main isoform in skeletal muscle. Presence of calumenin in rabbit sarcoplasmic reticulum (SR) was identified by Western blot analysis. GST-pull down and co-immunoprecipitation experiments showed that ryanodine receptor 1 (RyR1) interacted with calumenin-2 in millimolar  $\text{Ca}^{2+}$  concentration range. Experiments of gradual EF-hand deletions suggest that the second EF-hand domain is essential for calumenin binding to RyR1. Adenovirus-mediated overexpression of calumenin-2 in C2C12 myotubes led to increased caffeine-induced  $\text{Ca}^{2+}$  release, but decreased depolarization-induced  $\text{Ca}^{2+}$  release. Taken together, we propose that calumenin-2 in the SR lumen can directly regulate the RyR1 activity in  $\text{Ca}^{2+}$ -dependent manner.

© 2006 Elsevier Inc. All rights reserved.

**Keywords:** Calcium binding protein; CREC family; Reticulocalbin; Crocalbin; Cab45; Excitation–contraction coupling

The  $\text{Ca}^{2+}$ -binding CREC family including Cab45 [1], reticulocalbin [2], ERC-55 [3], calumenin [4–7], and crocalbin [8] has multiple EF-hands and a C-terminal ER retention signal. Unlike other EF-hand proteins, the CREC family possesses a low  $\text{Ca}^{2+}$  affinity with dissociation constants in millimolar range [5]. Calumenin identified first in mouse cardiac SR has 315 aa containing a N-terminal signal sequence, 6 EF-hands, and a unique

C-terminal ER/SR retention signal, HDEF [4]. Mouse and human calumenins were expressed ubiquitously in all tested tissues but were especially enriched in heart and lung [4,5,7]. In spite of the retrieval signal, HDEF for ER/SR, the localization of calumenin was less strict [9]. Although several results have been reported to suggest the possible relationship of calumenin with disease states [10–18], the functional roles of calumenin in ER/SR are largely unknown.

The excitation–contraction (E–C) coupling of skeletal muscle is a series of events in which a depolarization of plasma membrane permits a conformational change of dihydropyridine receptor (DHPR), which in turn release  $\text{Ca}^{2+}$  through RyR1 from SR and muscle contraction [19]. The sequential relaxation is initiated by re-uptake of intracellular  $\text{Ca}^{2+}$  through the action of sarcoplasmic/endoplasmic reticulum  $\text{Ca}^{2+}$ -ATPase (SERCA) [19]. Several integral membrane proteins, triadin and junctin, and the intraluminal  $\text{Ca}^{2+}$ -binding protein, calsequestrin,

☆ **Abbreviations:** aa, amino acid(s); Con-A, concanavalin A; 2-DE, two-dimensional electrophoresis; ECC, excitation-contraction coupling; DHPR, dihydropyridine receptor; ER, endoplasmic reticulum; GP, glycogen phosphorylase; GST, glutathione *S*-transferase; HRC, histidine-rich  $\text{Ca}^{2+}$ -binding protein; MALDI-TOF, matrix-assisted laser desorption ionization-time-of-flight; PCR, polymerase chain reaction; PFK, phosphofructokinase; RT, reverse transcription; RyR, ryanodine receptor; SERCA, sarcoplasmic/endoplasmic reticulum ATPase; SR, sarcoplasmic reticulum.

\* Corresponding author. Fax: +82 62 970 3414.

E-mail address: [dhkim@gist.ac.kr](mailto:dhkim@gist.ac.kr) (D.H. Kim).

were proposed to form a  $\text{Ca}^{2+}$  release complex with RyR1 and may regulate the functions of RyR [20–23]. Evidence also shows that the histidine-rich  $\text{Ca}^{2+}$ -binding protein (HRC) in the SR lumen could participate in the association with triadin and regulate the  $\text{Ca}^{2+}$  release process [24,25]. Recently, junctate, another high capacity  $\text{Ca}^{2+}$ -binding protein, has been cloned and identified as an integral SR luminal protein [26,27]. However, the functional role of junctate in the SR is largely unknown.

The present study was carried out to examine the roles of calumenin in rabbit skeletal SR. Our results show that calumenin-2, the major isoform in rabbit skeletal muscle interacts with RyR1 in millimolar  $\text{Ca}^{2+}$  concentration range. In addition, the over-expression of calumenin-2 in C2C12 cells altered RyR1-mediated  $\text{Ca}^{2+}$  transients. Therefore, we propose that calumenin-2 located in the skeletal SR lumen can directly regulate the activity of RyR1.

## Experimental procedures

**cDNA cloning of rabbit calumenins.** Total RNAs from rabbit heart (left ventricle) and skeletal muscles (fast twitch muscles of the hind-limbs) were isolated using Invisorb Spin Tissue RNA Mini Kit (Invitex), and subsequently cDNAs were synthesized using random hexamer/oligo(dT) and Omniscript reverse transcriptase (Qiagen). To clone rabbit calumenin cDNAs, two oligonucleotide primers were designed based on the highly conserved mouse and human calumenins (Figs. 1A and B). The forward primer was 5'-CCGGAATTCATCATGGACCTGCG-3' (*EcoRI* site, CCGGAATTCATC plus calumenin nucleotide, 1–11) and the reverse primer was 5'-CCGCTCGAGAGCTCAGAACTCATCATG-3' (*SacI* site, CCGCTCGAGAGC plus calumenin nucleotide, 934–948). PCR was performed with 35 cycles of 94 °C for 30 s, 60 °C for 60 s, and 72 °C for 120 s, with a GeneAmp2700 thermal cycler (Applied Biosystems). The PCR products were cloned into pCR<sup>®</sup>2.1-TOPO vectors (Invitrogen) and were sequenced on both strands by automated DNA sequencing using the ABI 3700 sequencer (Applied Biosystems).

**Isolation of rabbit skeletal SR vesicles.** Longitudinal and junctional SR vesicles were isolated from the predominantly fast twitch muscles of rabbit hind limbs and back by sucrose density gradient ultra-centrifugation as described previously [28].

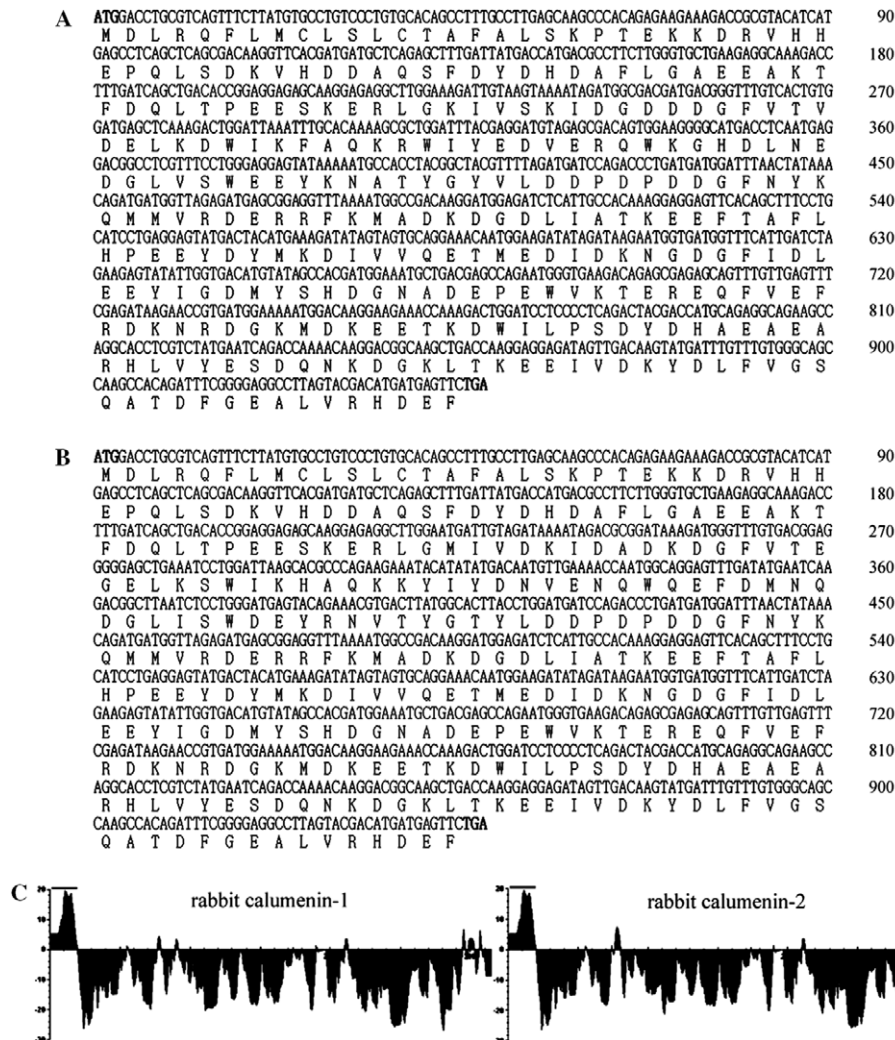


Fig. 1. cDNA cloning and analysis of the deduced aa sequences of rabbit calumenin genes. (A,B) The deduced aa sequences of rabbit calumenins. The start (ATG) and stop (TGA) condons in both calumenins (A: rabbit calumenin-1; B: rabbit calumenin-2) and the first methionine residues (M) are in boldface. (C) Hydropathy plots calculated by the algorithm of Kyte-Doolittle show that both calumenins have a typical amino-terminal signaling sequence (solid line) without any visible transmembrane sequence.

**GST fusion proteins and GST-pull-down assay.** All GST fusion proteins were generated using pGEX 4T-1 by the bacterial expression system [23]. For GST-pull-down assay, the junctional SR preparations were solubilized for 0.5 h at room temperature at a protein concentration of 2 mg/ml in 10 mM Tris-HCl (pH 7.4), 1.5% Triton X-100, 0.1 M NaCl, 1 mM dithiothreitol, and the protease inhibitor cocktail (Sigma-Aldrich) (solubilizing buffer) containing 2.5 mM CaCl<sub>2</sub>, and the supernatant was taken after centrifugation at 40,000 rpm in 45 Ti rotor (200,000g, Beckman) for 5 min to remove unsolubilized vesicles and precipitates. The supernatant was further incubated with glutathione-Sepharose beads for 1 h at 4 °C to remove non-specific beads binding materials. The supernatants were then incubated with native or truncated forms of GST-calumenin-2 (originally cloned from and substantially expressed in skeletal muscle cDNA, Fig. 2C) bound affinity matrices for 0.5 h at room temperature. The incubation and the following washing steps were done with 10 mM Tris-HCl (pH 7.4), 0.15% Triton X-100, 0.01 M NaCl, 1 mM dithiothreitol, and the protease

inhibitor cocktail (Sigma-Aldrich) containing the indicated concentration of CaCl<sub>2</sub> or EGTA.

**Co-immunoprecipitation.** The junctional SR vesicles were solubilized in the solubilizing buffer containing 2.5 mM CaCl<sub>2</sub> (see above). After centrifugation at 40,000 rpm in 45 Ti rotor (200,000g, Beckman) for 5 min to remove unsolubilized vesicles and precipitates, the supernatant was further cleared with protein A or G-agarose beads for 1 h at 4 °C. With anti-RyR1 (Affinity BioReagents) plus protein G-agarose beads or purified anti-calumenin antibodies and protein A agarose beads, the co-immunoprecipitation (co-IP) was carried out as previously described [24].

**Preparation of GST-calumenin-2 deletion mutants.** To prepare all GST fusion proteins having progressively deleted EF-hand Ca<sup>2+</sup>-binding domains, we cloned the calumenin-2 mutant cDNAs into pGEX 4T-1 and purified according to the manufacturer's manual (Amersham Biosciences).

**Cell culture, preparation of recombinant adenovirus, and intracellular Ca<sup>2+</sup> measurement in a single cell.** C2C12 myoblasts derived from mouse skeletal muscle were used as described previously [29]. The Adeno-X

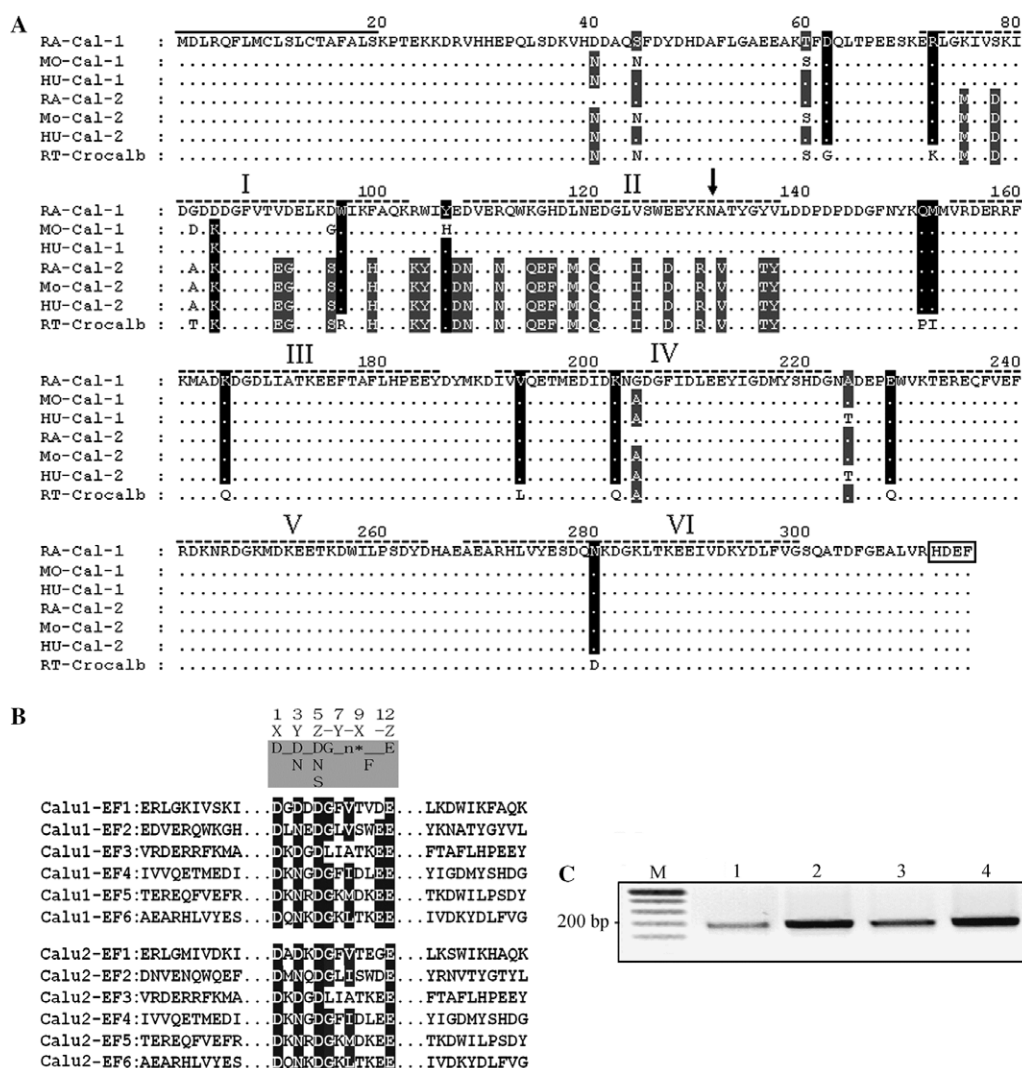


Fig. 2. Alignment of mammalian calumenins, predicted six EF-hand domains, and the isoform specific RT-PCR. (A) The deduced aa sequences of rabbit calumenin-1 (RA-Cal-1, GenBank Accession No. AY225335) and rabbit calumenin-2 (RA-Cal-2, GenBank Accession No. AY225336) were aligned with mouse calumenins (MO-Cal-1 and -2), human calumenins (HU-Cal-1 and -2), and rat crocalbin (RT-Crocalb). All aligned calumenins show a 19 aa N-terminal signal sequence (solid line), predicted six EF-hand domains (Roman numerals on dashed lines), and a unique ER/SR retention signal, HDEF (boxed). The vertical arrow indicates one N-glycosylation site (aa 131). Note that each isoform of calumenins shows the maximum difference in the first two EF-hand regions (aa 74–138). (B) The predicted 6 EF-hand domains of rabbit calumenin-1 (upper alignment) and -2 (lower alignment) were aligned with the consensus sequences. (C) The isoform specific expression levels of PCR products were analyzed using rabbit calumenin-1 (lanes 1 and 2) and -2 (lanes 2 and 3) specific primers and rabbit skeletal (lanes 1 and 3) and cardiac (lanes 2 and 4) cDNAs. The 194 bp RT-PCR products were run on 1% agarose gel with size marker (M).



expression system kit (Clontech) was used to generate rabbit calumenin-2 (AdCalu-2) and  $\beta$ -galactosidase (AdLac-Z) overexpressing adenoviruses [25]. Three days after infection with AdCalu-2 or AdLac-Z, intracellular  $\text{Ca}^{2+}$  transients in C2C12 myotubes were measured by addition of 10 mM caffeine or 20 mM KCl on coverslips after incubating for 45 min at 37 °C in a balanced salt solution (BBS) (140 mM NaCl, 2.8 mM KCl, 2 mM  $\text{CaCl}_2$ , 2 mM  $\text{MgCl}_2$ , and 10 mM Hepes, pH 7.2) containing 5  $\mu\text{M}$  Fura 2-AM as described previously [29].

## Results

### *cDNA cloning and analysis of the primary sequences of rabbit calumenins*

cDNA sequences and genomic organization of mouse and human calumenin isoforms have been characterized recently [7]. In the present study, we attempted to clone rabbit calumenin cDNAs by RT-PCR using total RNA obtained from rabbit cardiac and skeletal muscles, as described previously [7]. Two types of calumenin cDNAs were identified and the aa sequences were predicted on the basis of their cDNA sequences (Figs. 1 and 2). We have named the two isoforms as rabbit calumenin-1 (Fig. 1A, GenBank Accession No. AY225335) and rabbit calumenin-2 (Fig. 1B, GenBank Accession No. AY225336), respectively. Both rabbit calumenins showed 92% identity and 95% homology to each other and were 315 aa long with the calculated MW of 37,055 and 37,096 and *pI* of 4.26 and 4.24, respectively. The hydropathy plots indicate that both isoforms have a typical N-terminal signal sequence (solid lines), but no membrane anchoring domain (Fig. 1C). Despite a major difference in aa sequence ranging from 74 to 137, where the first two putative EF-hand domains reside (Fig. 2A), both rabbit calumenins have a 19 aa N-terminal signal sequence (Fig. 2A, solid line), putative 6 EF-hands (Fig. 2A, Roman numerals on dashed lines), a N-glycosylation site at 131 aa (Fig. 2A, arrow), and a 4 aa C-terminal ER/SR retention sequence, HDEF (Fig. 2A, boxed) (predicted by two computer software programs, InterPro, <http://www.ebi.ac.uk/interpro/> and Pfam, <http://www.sanger.ac.uk/Software/Pfam/>).

The consensus sequence predicting the aligned six putative EF-hand domains in the rabbit calumenin isoforms is shown in Fig. 2B. Except for the substitutions of Leu for Gly (aa 169) in the  $\text{Ca}^{2+}$ -binding loop of both third EF-hands, most residues in the loops resemble the consensus (Fig. 2B). Although isoform specific RT-PCR showed that the rabbit calumenin-1 and -2 were simultaneously present at rabbit skeletal (Fig. 2C, lanes 1 and 3) and cardiac (Fig. 2C, lanes 2 and 4) tissues, rabbit calumenin-2 originally cloned from skeletal muscle cDNA was the major form of calumenin in rabbit skeletal muscle and was used for further studies.

### *Identification of calumenin in skeletal SR membranes*

In light of the evidence that calumenin has a C-terminal ER retention signal [4–7], we examined the presence of

calumenin in two fractions of rabbit skeletal SR representing the longitudinal and junctional SR fractions by Western blot analysis. The 52.5 kDa calumenin was identified in the junctional SR fraction (Fig. 3B, lane 2), where RyR1, triadin, FKBP12 (Fig. 3B, lane 2), and calsequestrin (Fig. 3, the 2nd arrow) are enriched.

### *GST-calumenin-2 interacts with RyR1 in the presence of millimolar $\text{Ca}^{2+}$*

In order to identify calumenin-binding proteins in the junctional SR, GST-pull down assay was conducted using GST-calumenin-2 and Triton X-100-solubilized junctional SR proteins in various  $\text{Ca}^{2+}$  concentrations, and the GST-calumenin-2 binding fractions were run on 10% SDS-PAGE gel (Fig. 4B). Mainly, three proteins having molecular weights of approximately 500, 100, and 87.5 kDa (Fig. 4B, arrows) were identified as GST-calumenin-2 interacting proteins. The 500 kDa protein was identified as RyR1 by immunoblotting with anti-RyR1 antibody in 6% SDS-PAGE (Fig. 4A). The 100 and 87.5 kDa proteins shown by the 2nd and 3rd arrows in Fig. 4A were identified as glycogen phosphorylase (GP) and phosphofructokinase 1 (PFK-I), respectively, by MALDI-TOF mass spectroscopy [30] (data not shown).

### *Co-immunoprecipitation of calumenin-2 with RyR1*

To confirm the interaction between calumenin-2 and RyR1 as shown by GST-pull down assay (Fig. 4), co-IP of RyR1 with calumenin-2 was also conducted using

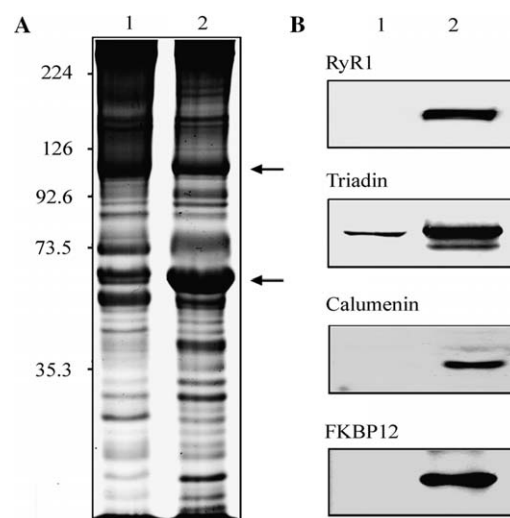


Fig. 3. Calumenin is enriched in the junctional rabbit skeletal SR preparation. (A) Coomassie blue staining of longitudinal (lane 1) and junctional rabbit skeletal SR (lane 2) proteins (20  $\mu\text{g}$ ) separated by 10% SDS-PAGE. The arrows indicate the bands of SERCA (upper) and calsequestrin (lower). (B) Western blot experiment for the longitudinal (lane 1) and junctional SR (lane 2) was conducted using the antibodies against RyR1, triadin, calumenin, and FKBP12 and NC blots electrically transferred from duplicated PAGE gel. Note that calumenin was enriched in the junctional SR preparations.

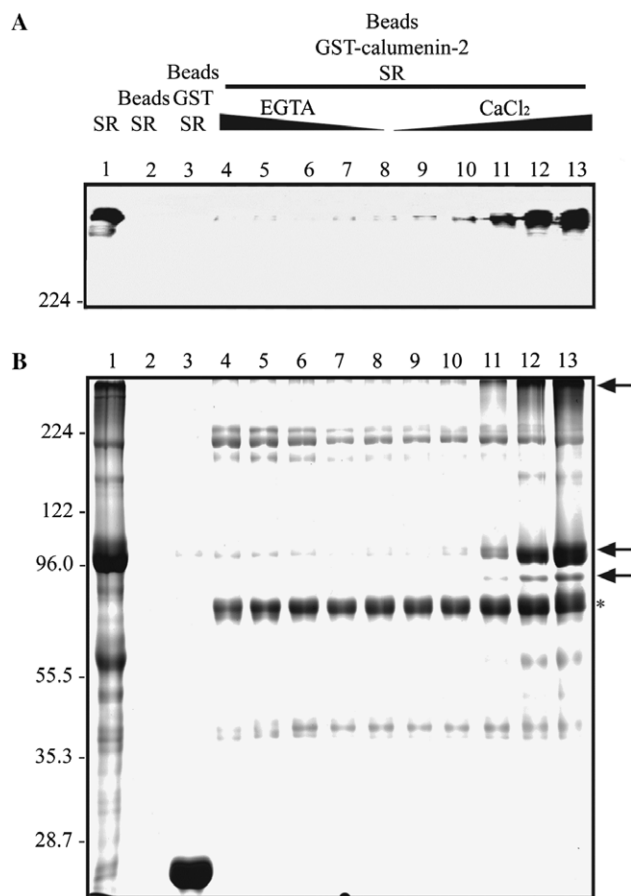


Fig. 4. Identification of GST-calumenin-2 binding proteins in the junctional SR by GST-pull down assay. (A) Western blot result showing the interaction between GST-calumenin-2 and RyR1. 1.5% Triton X-100-solubilized junctional SR proteins (lane 1), solubilized junctional SR proteins bound to glutathione-Sepharose beads (lane 2), solubilized junctional SR proteins bound to GST immobilized on glutathione-Sepharose beads (lane 3), and the solubilized junctional SR proteins bound to GST-calumenin-2 immobilized glutathione-Sepharose beads in the presence of 10 mM EGTA (lane 4), 5 mM EGTA (lane 5), 1 mM EGTA (lane 6), 0.1 mM EGTA (lane 7), no EGTA (lane 8), 0.01 mM CaCl<sub>2</sub> (lane 9), 0.1 mM CaCl<sub>2</sub> (lane 10), 1 mM CaCl<sub>2</sub> (lane 11), 2.5 mM CaCl<sub>2</sub> (lane 12), and 5 mM CaCl<sub>2</sub> (lane 13) were separated in 6% SDS-PAGE and electrically transferred to NC membrane. Western blot experiment was conducted using anti-RyR1 antibody. (B) Coomassie blue-stained gel to show the GST-calumenin-2 binding proteins in the junctional SR. The same GST-pull down products as shown in (A) were separated in 10% SDS-PAGE and stained by Coomassie blue. The arrows indicate the GST-calumenin-2 interacting 500 kDa RyR1 verified by Western blot as shown in (A), and 100 kDa GP and 87.5 kDa FPK-1 proteins which were identified by MALDI-TOF mass spectroscopy, respectively. The interactions between GST-calumenin-2 and each of the three proteins were markedly enhanced by increased Ca<sup>2+</sup> concentration. The asterisk verifies that the same amount of GST-calumenin-2 was used for the experiment.

anti-calumenin and anti-RyR1 antibodies with Triton X-100-solubilized junctional SR proteins in the presence of 2.5 mM CaCl<sub>2</sub> (Fig. 5). Calumenin was immunoprecipitated by anti-calumenin antibody as well as by anti-RyR1 antibody (Fig. 5A). RyR1 was also immunoprecipitated by anti-RyR1 antibody as well as by anti-calumenin antibody (Fig. 5B). It is interesting to note that the interactions

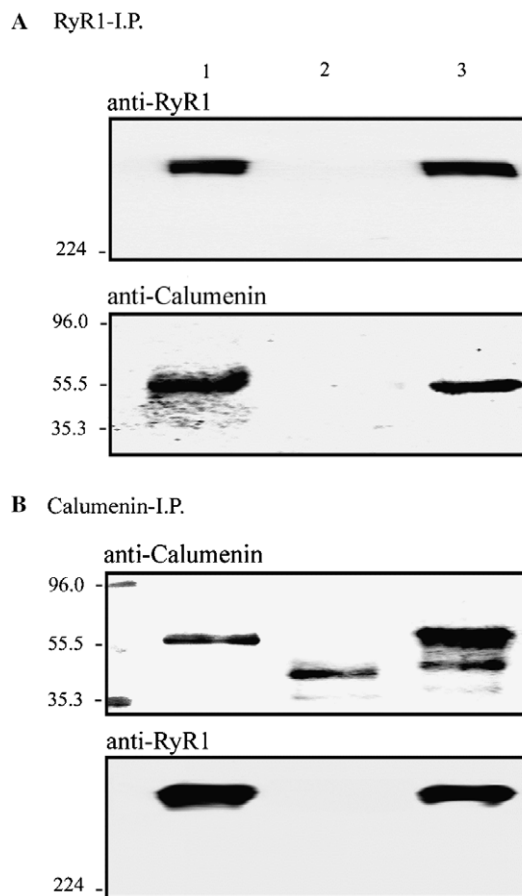


Fig. 5. Co-immunoprecipitation of calumenin-2 and RyR1. Triton X-100-solubilized junctional SR proteins (20 µg) (lane 1), immunoprecipitated proteins with preimmune serum (mouse and rabbit preimmune serums for A and B, respectively) (lane 2) and immunoprecipitated proteins with anti-RyR1 (A) or anti-calumenin (B) antibodies in the presence of 2.5 mM CaCl<sub>2</sub> (lane 3) were separated either in 6% (for RyR1 IP) or 10% (for calumenin IP) SDS-PAGE. (A) Immunoprecipitated proteins with anti-RyR1 antibody were probed with anti-RyR1 (A, upper panel) or with anti-calumenin antibody (A, lower panel). (B) Immunoprecipitated proteins with anti-calumenin antibody were probed with anti-calumenin (B, upper panel) or with anti-RyR1 (B, lower panel) antibodies. Asterisks indicate a non-specific immunoreactive band formed by rabbit IgG against the anti-calumenin antibody.

were completely abolished in the presence of 2.5 mM EGTA (data not shown).

#### Identifying RyR1 interacting domain in calumenin-2

To identify the putative RyR1 binding domain in GST-calumenin-2, six EF-hand domains were progressively deleted (Figs. 6A and B), and GST-pull down assay was conducted using Triton X-100-solubilized SR vesicles, and RyR1 binding was examined by Western blot assay using anti-RyR1 antibody. Densitometric scanning (Fig. 6D) of the Western blot results shown in Fig. 6C revealed that the interaction between GST-calumenin-2 and RyR1 increased markedly by the presence of the second EF-hand domain (71% of the maximal binding),

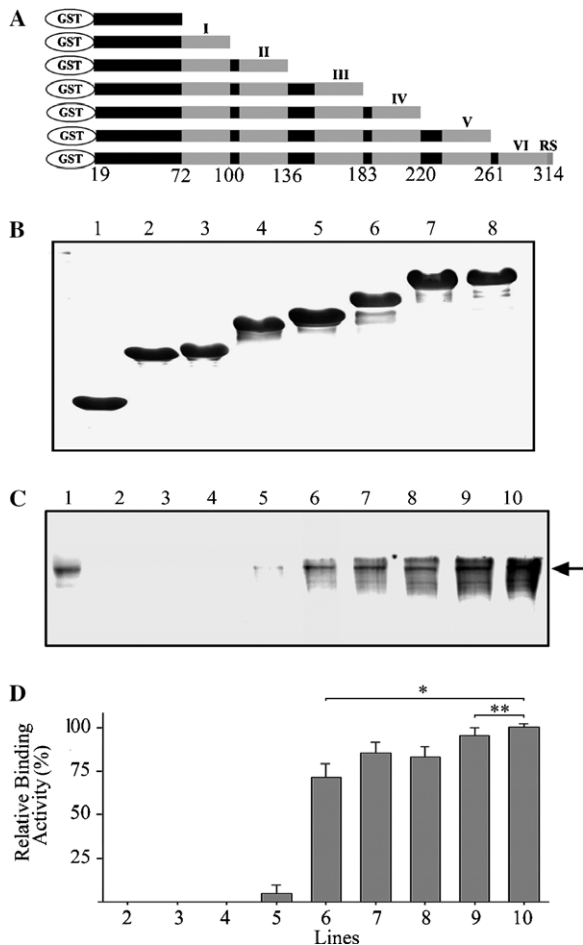


Fig. 6. Effects of deletion-mutation on the interactions between GST-calumenin-2 and RyR1. (A) Progressive deletion of EF-hand domains from the direction of C-terminal end was conducted in GST-calumenin-2 fusion proteins. RS stand for the retention signal and the Roman numerals indicate the predicted six EF-hand domains. (B) GST control (lane 1), GST-calumenin-2 without entire EF-hand domains (lane 2), and GST-calumenin-2 mutants having different number of EF-hand (lanes 3–8) were expressed and purified from *Escherichia coli* (BL21), and were separated in 10% SDS–PAGE gel. (C) Triton X-100-solubilized junctional SR proteins (lane 1), solubilized junctional SR proteins bound to glutathione–Sepharose beads (lane 2), solubilized junctional SR proteins bound to GST immobilized on glutathione–Sepharose beads (lane 3), solubilized junctional SR proteins bound to GST-calumenin-2 without the EF-hand domains immobilized on glutathione–Sepharose beads (lane 4), and solubilized junctional SR proteins bound to mutant GST-calumenin-2 having different number of EF-hand domains (lanes 5–10) immobilized on glutathione–Sepharose beads as shown in (B) were separated in 6% SDS–PAGE and were subjected to immunoblotting with anti-RyR1 antibody. All the interactions were conducted in the presence of 5 mM  $\text{CaCl}_2$ . (D) Relative RyR1 binding of the serially EF-hand deleted GST-calumenin-2 as shown in (C) was analyzed by densitometric scanning and background subtraction. The averaged values from three different experiments are shown as means  $\pm$  SD in a bar graph. \* denotes the difference from GST-calumenin-2 having only first EF-hand domain at  $P < 0.05$ ; \*\* denotes the difference from GST-calumenin-2 having the first two EF-hand domains at  $P < 0.05$  according to ANOVA analysis.

suggesting that the RyR1 binding site in calumenin-2 resides in the 2nd EF-hand region. However, the result of further increase of binding by the 5th and 6th EF-hand domains (Fig. 6D) implies that the structural integrity of

calumenin formed by the six EF-hands is important for the full binding affinity between calumenin-2 and RyR1.

#### Overexpression of calumenin-2 alters intracellular $\text{Ca}^{2+}$ transients in C2C12 cells

To determine whether calumenin plays any role in the intracellular  $\text{Ca}^{2+}$  transients, caffeine- and depolarization-induced  $\text{Ca}^{2+}$  release was measured in the AdCalu-2-infected calumenin-2 overexpressing C2C12 myotubes. About 7.5-fold increase of calumenin-2 expression was obtained 3 days after infection with AdCalu-2 (Fig. 7E). The peak amplitude of the caffeine-induced  $\text{Ca}^{2+}$  release was significantly increased in the AdCalu-2-infected C2C12 myotubes ( $2.88 \pm 0.26$ ,  $n = 14$ ) than in the non-infected ( $1.83 \pm 0.21$ ,  $n = 7$ ) or AdLac-Z infected C2C12 myotubes ( $2.13 \pm 0.22$ ,  $n = 12$ ), suggesting that the SR  $\text{Ca}^{2+}$  storage capacity increased in the AdCalu-2-infected C2C12 myotubes (Figs. 7A and C). In contrast to the caffeine-induced  $\text{Ca}^{2+}$  release from the SR, the peak amplitude of the depolarization-induced  $\text{Ca}^{2+}$  release in AdCalu-2-infected C2C12 myotubes was slightly but significantly lower ( $2.15 \pm 0.15$ ,  $n = 13$ ; in 2 cases out of 13 experiments the values were similar to AdLac-Z-infected or non-infected C2C12 myotubes) than in non-infected ( $2.41 \pm 0.17$ ,  $n = 9$ ) or AdLac-Z-infected C2C12 myotubes ( $2.46 \pm 0.11$ ,  $n = 14$ ) (Figs. 7B and D), suggesting that calumenin-2 has inhibitory effect on RyR1 under the physiological stimuli.

#### Discussion

In the present study, we cloned two rabbit calumenin isoforms (calumenin-1 and calumenin-2) having a 19 aa N-terminal signal sequence and a 4 aa C-terminal ER/SR retention sequence, HDEF. We have further studied the role of calumenin in E–C coupling of rabbit skeletal SR. The novel findings in this study are: (1) calumenin-2 can directly interact with RyR1 in millimolar  $\text{Ca}^{2+}$  concentration range, (2) the binding site of RyR1 in calumenin-2 is in the 2nd EF-hand region, and (3) calumenin-2 can influence RyR1-mediated  $\text{Ca}^{2+}$  release from SR. Therefore, we postulate that calumenin-2 having relatively low  $\text{Ca}^{2+}$ -binding affinity ( $K_d \sim 0.6$  mM) is located in the lumen of junctional SR and regulates the physiological  $\text{Ca}^{2+}$  release from the SR. Calumenin can be considered as a unique SR resident protein [4–7] because of its multiple EF-hand repeats unlike the other  $\text{Ca}^{2+}$ -binding proteins in the SR, e.g., HRC, sarcalumenin, calsequestrin, and calreticulin [22].

Both mouse and human calumenin genes have high similarities in the genomic organization resulting from the alternative second exon transcription [7]. The restricted difference between the two rabbit calumenin isoforms also resides in the first two EF-hand domains (Fig. 2A), suggesting that the genomic organization of rabbit calumenin genes is identical to that of mouse and human [7]. In sequence analysis, although another primary sequence

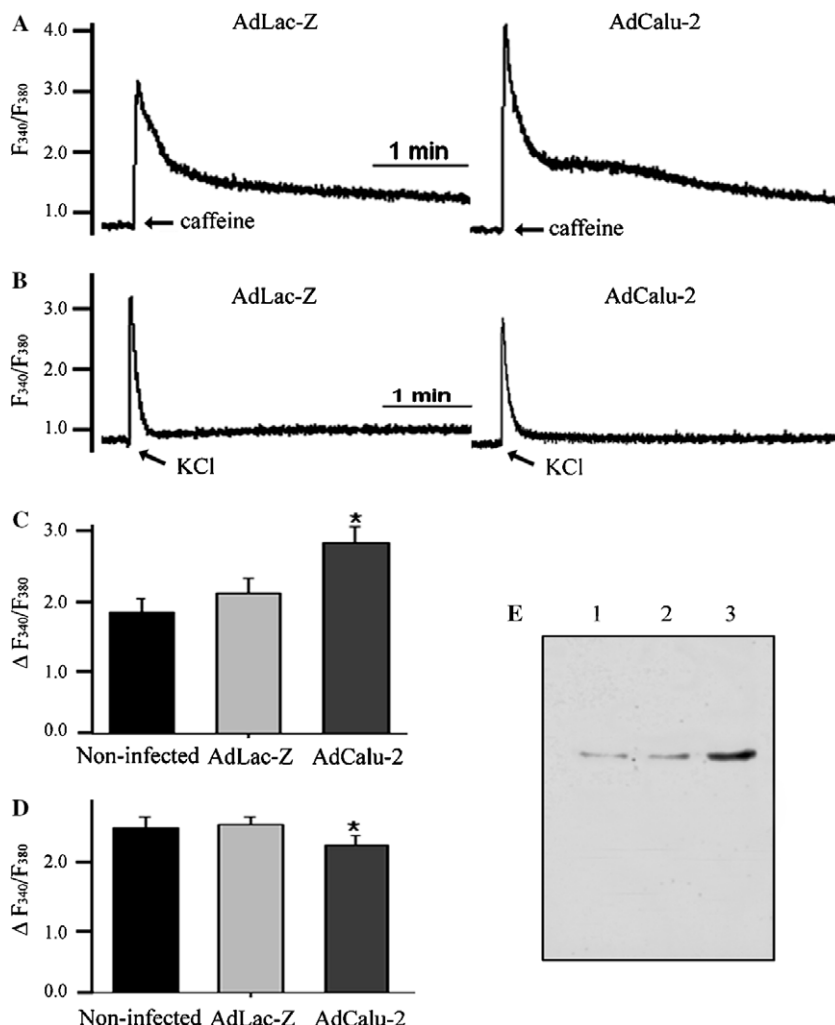


Fig. 7. Altered intracellular  $\text{Ca}^{2+}$  transients in C2C12 myotubes overexpressing calumenin-2. (A) C2C12 myotubes were infected with either adenovirus overexpressing  $\beta$ -galactosidase (AdLac-Z) or adenovirus overexpressing calumenin-2 (AdCalu-2) and were cultured for three more days. Intracellular  $\text{Ca}^{2+}$  release was induced by 10 mM caffeine in the presence of 2 mM extracellular  $\text{Ca}^{2+}$ . (B) Intracellular  $\text{Ca}^{2+}$  releases were induced by 20 mM KCl in the presence of 2 mM extracellular  $\text{Ca}^{2+}$ . (C,D) The averaged values of multiple experiments shown in A and B were presented as means  $\pm$  SD in bar graphs, respectively. According to ANOVA, significantly higher caffeine-induced but significantly lower depolarization-induced  $\text{Ca}^{2+}$  release in AdCalu-2 infected C2C12 myotubes was identified (\* $P < 0.05$  versus non-infected or AdLac-Z infected C2C12 myotubes). (E) The overexpression of calumenin in AdCalu-2 infected C2C12 myotubes (lane 3) was compared with non-infected (lane 1) or AdLac-Z infected (lane 2) C2C12 myotubes by immunoblotting with purified anti-calumenin antibody. Densitometric scanning shows that  $\sim 7.5$ -fold overexpression of calumenin-2 in AdCalu-2 infected C2C12 myotubes.

region (aa 36–67) was speculated as an EF-hand domain in both calumenin isoforms, we excluded the region from the functional ones because of the two substitutions, Ala (aa 51) for Gly and Gly (aa 54) for one of the other preferred residues in the  $\text{Ca}^{2+}$ -binding motif. Interestingly, we found a conserved substitution of Leu (aa 169) for Gly serving as a hinge region in the  $\text{Ca}^{2+}$ -binding motif from all tested species (Figs. 2A and B). Structural explanations for the relationship between the identified primary sequences and the reported low  $\text{Ca}^{2+}$  affinity of calumenin [5] have remained to be elucidated.

The RyR1-binding site in calumenin-2 and the possible involvement of the different EF-hand domains in the binding between RyR-1 and calumenin-2 were examined by the serial deletion mutations shown in Fig. 6. There were largely two transitions in the binding. The major one was the

$\sim 70\%$  increase in the binding between calumenin-2 and RyR1 when the 2nd EF-hand region was added to the GST-construct (II). Therefore, the RyR1 binding site in calumenin-2 is most likely in the 2nd EF-hand region. The minor transitional increase ( $\sim 30\%$ ) was seen when the 5th EF-hand region was included in the GST-construct, indicating that the 5th EF-hand region could be critical for the full gaining of binding affinity between the two proteins.

The GST-calumenin-2 also interacted with the 100 kDa GP protein in the Triton X-100-solubilized junctional SR in  $\text{Ca}^{2+}$ -dependent manner (Fig. 5B, middle arrow). The functional roles of GP in the striated muscle SR have not been well studied. However, it is interesting to note that GP would be a reversible effector of mastoparan which affects the RyR1-mediating  $\text{Ca}^{2+}$  release pro-



cess [31,32]. Therefore, it is tempting to speculate that the complex formation among calumenin-2, GP, and RyR1 may play a role in the regulation of  $\text{Ca}^{2+}$  release from the skeletal SR (Fig. 4B). However, the study concerning the role of GP in E–C coupling is beyond the scope of this study.

The functional role of calumenin in the junctional SR was further studied by examining caffeine or depolarization-induced  $\text{Ca}^{2+}$  release from SR in the control and calumenin-overexpressed C2C12 myotubes (Fig. 7). There was a significant increase in caffeine-induced  $\text{Ca}^{2+}$  release, but decrease in depolarization-induced  $\text{Ca}^{2+}$  release from the SR in the differentiated C2C12 myotubes harboring overexpressed calumenin-2 (Fig. 7). The increased caffeine-induced  $\text{Ca}^{2+}$  release upon calumenin-2 overexpression was likely due to the increased  $\text{Ca}^{2+}$  storage capacity in the SR by overexpressed calumenin, as shown in other luminal  $\text{Ca}^{2+}$ -binding proteins such as calsequestrin [33,34] and HRC [25,35]. On the other hand, the apparent decrease of depolarization-induced  $\text{Ca}^{2+}$  release may be due to: (a) a direct interaction of RyR1 with the overexpressed calumenin-2; (b) increased SR  $\text{Ca}^{2+}$ -buffering capacity leading to lower intraluminal free  $\text{Ca}^{2+}$  concentrations, which is associated with the lower amounts of  $\text{Ca}^{2+}$  release. Similar observations were reported previously in calsequestrin-overexpressed transgenic mice [31].

The implications of calumenin in cardiac pathogenesis have been reported. An increased expression of calumenin was reported to be proportional to the progress of human idiopathic dilated cardiomyopathy (IDCM) [14]. IDCM was characterized by a significant decrease in SR  $\text{Ca}^{2+}$  release even under the large amount of  $\text{Ca}^{2+}$  sustained in the SR [36]. The abnormal gating mechanism of  $\text{Ca}^{2+}$  release channel/RyR in response to stimuli could lead to about 50% decrease in contractility [36]. However, the underlying mechanisms for the  $\text{Ca}^{2+}$  release dysfunction in DCM are poorly understood. Observations of the sustained  $\text{Ca}^{2+}$  overload caused by defects in RyR gating [36] and the progressively increased calumenin expression [13] along with our present finding showing the inhibitory role of calumenin on depolarization-induced  $\text{Ca}^{2+}$  release suggest that the  $\text{Ca}^{2+}$ -dependent inhibitory role of calumenin to RyR2 may be the cause for the pathogenesis of the disease.

In the present study, we show evidence that calumenin, the six EF-hand protein located in the SR lumen, could participate in the  $\text{Ca}^{2+}$  cycling via SR by the  $\text{Ca}^{2+}$ -dependent interaction with RyR1.

## Acknowledgments

We thank Dr. R. Wallin for supplying us with the anti-calumenin polyclonal antibody. This work was supported by grants from the Korea Ministry of Science and Technology (Systems Biology Research Grant, M1-0309-00-0006),

Korea Science and Engineering foundation (Basic Research Program 1999-1-20700-002-5), and Ministry of Education (Brain Korea 21 Project).

## References

- [1] P.E. Scherer, G.Z. Lederkremer, S. Williams, M. Fogliano, G. Baldini, H.F. Lodish, Cab45, a novel Ca-binding protein localized to the Golgi lumen, *J. Cell. Biol.* 133 (1996) 257–268.
- [2] M. Ozawa, T. Muramatsu, Reticulocalbin, a novel endoplasmic reticulum resident Ca-binding protein with multiple EF-hand motifs and a carboxyl-terminal HDEL, *J. Biol. Chem.* 268 (1993) 699–705.
- [3] K. Weis, G. Griffiths, A. Lamond, The endoplasmic reticulum calcium-binding protein of 55 kDa is a novel EF-hand protein retained in the endoplasmic reticulum by a carboxyl-terminal His-Asp-Glu-Leu motif, *J. Biol. Chem.* 269 (1994) 19142–19150.
- [4] D. Yabe, T. Nakamura, N. Kanazawa, K. Tashiro, T. Honjo, Calumenin, a  $\text{Ca}^{2+}$ -binding protein retained in the endoplasmic reticulum with a novel carboxyl-terminal sequence, HDEF, *J. Biol. Chem.* 272 (1997) 18232–18239.
- [5] H. Vorum, X. Liu, P. Madsen, H.H. Rasmussen, B. Honore, Molecular cloning of a cDNA encoding human calumenin, expression in *Escherichia coli* and analysis of its  $\text{Ca}^{2+}$ -binding activity, *Biochim. Biophys. Acta.* 1386 (1998) 121–131.
- [6] D. Yabe, M. Taniwaki, T. Nakamura, N. Kanazawa, K. Tashiro, T. Honjo, Human calumenin gene (CALU): cDNA isolation and chromosomal mapping to 7q32, *Genomics* 49 (1998) 331–333.
- [7] D.H. Jung, D.H. Kim, Characterization of isoforms and genomic organization of mouse calumenin, *Gene* 327 (2004) 185–194.
- [8] M.J. Hseu, C.H. Yen, M.C. Tzeng, Crocalbin: a new calcium-binding protein that is also a binding protein for clotoxin, a neurotoxic phospholipase A2, *FEBS Lett.* 445 (1999) 440–444.
- [9] H. Vorum, H. Hager, B.M. Christensen, S. Nielsen, B. Honore, Human calumenin localizes the secretory pathway and is secreted to the medium, *Exp. Cell Res.* 248 (1999) 473–481.
- [10] H. Vorum, C. Jacobsen, B. Honore, Calumenin interacts with serum amyloid P component, *FEBS Lett.* 465 (2000) 129–134.
- [11] R. Wallin, S.M. Hutson, D. Cain, A. Sweatt, D.C. Sane, A molecular mechanism for genetic warfarin resistance in the rat, *FASEB J.* 15 (2001) 2542–2544.
- [12] N.N. Khodarev, J.O. Park, J. Yu, N. Gupta, E. Nodzenski, B. Roizman, R.R. Weichselbaum, Dose-dependent and independent temporal patterns of gene responses to ionizing radiation in normal and tumor cells and tumor xenografts, *Proc. Natl. Acad. Sci. USA* 98 (2001) 12665–12670.
- [13] W. Wu, X. Tang, W. Hu, R. Lotan, W.K. Hong, L. Mao, Identification and validation of metastasis-associated proteins in head and neck cancer cell lines by two-dimensional electrophoresis and mass spectrometry, *Clin. Exp. Metastasis* 19 (2002) 319–326.
- [14] R. Grzeskowiak, H. Witt, M. Drungowski, R. Thermann, S. Hennig, A. Perrot, K.J. Osterziel, D. Klingbiel, S. Scheid, R. Spang, H. Lehrach, P. Ruiz, Expression profiling of human idiopathic dilated cardiomyopathy, *Cardiovasc. Res.* 59 (2003) 400–411.
- [15] J.A. Coppinger, G. Cagney, S. Toomey, T. Kislinger, O. Belton, J.P. McRedmond, D.J. Cahill, A. Emili, D.J. Fitzgerald, P.B. Maguire, Characterization of the proteins released from activated platelets leads to localization of novel platelet proteins in human atherosclerotic lesions, *Blood* 103 (2003) 2096–2104.
- [16] N. Wajih, D.C. Sane, S.M. Hutson, R. Wallin, The inhibitory effect of calumenin on the vitamin K-dependent gamma-carboxylation system. Characterization of the system in normal and warfarin-resistant rats, *J. Biol. Chem.* 279 (2004) 25276–25283.
- [17] S.J. Ding, Y. Li, X.X. Shao, H. Zhou, R. Zeng, Z.Y. Tang, Q.C. Xia, Proteome analysis of hepatocellular carcinoma cell strains, MHCC97-H and MHCC 97-L, with different metastasis potentials, *Proteomics* 4 (2004) 982–994.



- [18] Y. Pan, T. Kislinger, A.O. Gramolini, E. Zvaritch, E.G. Kranias, D.H. MacLennan, A. Emili, Identification of biochemical adaptations in hyper- or hypocontractile hearts from phospholamban mutant mice by expression proteomics, *Proc. Natl. Acad. Sci. USA* 101 (2004) 2241–2246.
- [19] C. Franzini-Armstrong, A.O. Jorgensen, Structure and development of E-C coupling units in skeletal muscle, *Annu. Rev. Physiol.* 56 (1994) 509–534.
- [20] C. Franzini-Armstrong, F. Protasi, Ryanodine receptors of striated muscles: a complex channel capable of multiple interactions, *Physiol. Rev.* 77 (1997) 699–729.
- [21] L. Zhang, J. Kelly, G. Schmeisser, Y.M. Kobayashi, L.R. Jones, Complex formation between junction, triadin, calsequestrin, and the ryanodine receptor. Proteins of the cardiac junctional sarcoplasmic reticulum membrane, *J. Biol. Chem.* 272 (1997) 23389–23397.
- [22] J.J. Mackrill, Protein-protein interactions in intracellular  $\text{Ca}^{2+}$  release channel function, *Biochem. J.* 337 (1999) 345–361.
- [23] J.M. Lee, S.H. Rho, D.W. Shin, C. Cho, W.J. Park, S.H. Eom, J. Ma, D.H. Kim, Negatively charged amino acids within the intraluminal loop of ryanodine receptor are involved in the interaction with triadin, *J. Biol. Chem.* 279 (2004) 6994–7000.
- [24] H.G. Lee, H. Kang, D.H. Kim, W.J. Park, Interaction of HRC (histidine-rich  $\text{Ca}^{2+}$  binding protein) and triadin in the lumen of sarcoplasmic reticulum, *J. Biol. Chem.* 276 (2001) 39533–39538.
- [25] E. Kim, D.W. Shin, C.S. Hong, D. Jeong, D.H. Kim, W.J. Park, Increased  $\text{Ca}^{2+}$  storage capacity in the sarcoplasmic reticulum by overexpression of HRC (histidine-rich  $\text{Ca}^{2+}$  binding protein), *Biochem. Biophys. Res. Commun.* 300 (2003) 192–196.
- [26] S. Treves, G. Feriotto, L. Moccagatta, R. Gambari, F. Zorzato, Molecular cloning, expression, functional characterization, chromosomal localization, and gene structure of juncate, a novel integral calcium binding protein of sarco(endo)plasmic reticulum membrane, *J. Biol. Chem.* 275 (2005) 39555–39568.
- [27] C.-S. Hong, M.-C. Cho, Y.-G. Kwak, C.H. Song, Y.-H. Lee, J.S. Lim, Y.K. Kwon, S.-W. Chae, D.H. Kim, Cardiac remodeling and atrial fibrillation in transgenic mice overexpressing junctin, *FASEB J.* 16 (2002) 1310–1312.
- [28] R.D. Mitchell, P. Palade, S. Fleischer, Purification of morphologically intact triad structures from skeletal muscle, *J. Cell Biol.* 96 (1983) 1008–1016.
- [29] D.W. Shin, Z. Pan, E.K. Kim, J.M. Lee, M.B. Bhat, J. Parness, D.H. Kim, J. Ma, A retrograde signal from calsequestrin for the regulation of store-operated  $\text{Ca}^{2+}$  entry in skeletal muscle, *J. Biol. Chem.* 278 (2003) 3286–3292.
- [30] A. Shevchenko, M. Wilm, O. Vorm, M. Mann, Mass spectrometric sequencing of proteins silver-stained polyacrylamide gels, *Anal. Chem.* 68 (1996) 850–858.
- [31] I.E. Andreeva, V.F. Makeeva, B.I. Kurganov, N.A. Chebotareva, N.B. Livanova, A tentative mechanism of the ternary complex formation between phosphorylase kinase, glycogen phosphorylase b and glycogen, *FEBS Lett.* 445 (1999) 173–176.
- [32] Y. Hirata, M. Atsumi, Y. Ohizumi, N. Nakahata, Mastoparan binds to glycogen phosphorylase to regulate sarcoplasmic reticular  $\text{Ca}^{2+}$  release in skeletal muscle, *Biochem. J.* 371 (2003) 81–88.
- [33] Y. Sato, D.G. Ferguson, H. Sako, G.W. Dorn 2nd, V.J. Kadamby, A. Yatani, B.D. Hoit, R.A. Walsh, E.G. Kranias, Cardiac-specific overexpression of mouse cardiac calsequestrin is associated with depressed cardiovascular function and hypertrophy in transgenic mice, *J. Biol. Chem.* 273 (1998) 28470–28477.
- [34] W. Wang, L. Cleemann, L.R. Jones, M. Morad, Modulation of focal and global  $\text{Ca}^{2+}$  release in calsequestrin-overexpressing mouse cardiomyocytes, *J. Physiol.* 524 (2000) 399–414.
- [35] G.C. Fan, K.N. Gregory, W. Zhao, W.J. Park, E.G. Kranias, Regulation of myocardial function by histidine-rich, calcium-binding protein, *Am. J. Physiol.* 287 (2004) H1705–H1711.